Structural Engineering and Mechanics, Vol. 34, No. 6 (2010) 719-738
DOI: http://dx.doi.org/10.12989/sem.2010.34.6.719

Influence of lateral motion of cable stays on cable-stayed bridges

P.H. Wang*, M.Y. Liu, Y.T. Huang and L.C. Lin

Department of Civil Engineering, Chung-Yuan University, Chung-Li, Taiwan, R.O.C.

(Received July 18, 2008, Accepted December 28, 2009)

Abstract. The aim of this paper concerns with the nonlinear analysis of cable-stayed bridges including the vibration effect of cable stays. Two models for the cable stay system are built up in the study. One is the OECS (one element cable system) model in which one single element per cable stay is used and the other is MECS (multi-elements cable system) model, where multi-elements per cable stay are used. A finite element computation procedure has been set up for the nonlinear analysis of such kind of structures. For shape finding of the cable-stayed bridge with MECS model, an efficient computation procedure is presented by using the two-loop iteration method (equilibrium iteration and shape iteration) with help of the catenary function method to discretize each single cable stay. After the convergent initial shape of the bridge is found, further analysis can then be performed. The structural behaviors of cable-stayed bridges influenced by the cable lateral motion will be examined here detailedly, such as the static deflection, the natural frequencies and modes, and the dynamic responses induced by seismic loading. The results show that the MECS model offers the real shape of cable stays in the initial shape, and all the natural frequencies and modes of the bridge including global modes and local modes. The global mode of the bridge consists of coupled girder, tower and cable stays motion and is a coupled mode, while the local mode exhibits only the motion of cable stays and is uncoupled with girder and tower. The OECS model can only offers global mode of tower and girder without any motion of cable stays, because each cable stay is represented by a single straight cable (or truss) element. In the nonlinear seismic analysis, only the MECS model can offer the lateral displacement response of cable stays and the axial force variation in cable stays. The responses of towers and girders of the bridge determined by both OECS- and MECS-models have no great difference.

Keywords: cable-stayed bridge; cable stays; catenary; OECS; MECS.

1. Introduction

Due to developments in the fields of computer technology, high strength steel cables, orthotropic steel decks and construction technology, rapid progress in the analysis and construction of cable-stayed bridges has been made in the last half century (Leonhardt and Zellner 1991, Gimsing 1997). Because of its aesthetic appeal, economic grounds and ease of erection, the cable-stayed bridge is considered as the most suitable construction type for mid- and large bridges spanning from 200 m to about 1000 m. The Tatara Bridge across the Seto Inland Sea, linking the main islands Honshu and Shikoku in Japan was the world's longest cable-stayed bridge before 2008. The Tatara Bridge

*Corresponding author, Professor, E-mail: phwang@cycu.edu.tw

was opened in May 1, 1999 and has a center span of 890 m and a total length of 1480 m. The tallest cable-stayed bridge in the world, Millau Viaduct with the tallest pier 341 m tall and roadway 270 m high, spanning the Tarn River in France has been completed in December 2004. Millau Viaduct has a total length of 2460 m with seven towers and eight spans. The bridge has the longest cable-stayed suspended deck in the world. The Sutong Bridge crossing the Yangtze River in China is newly completed in June 2008 and includes a cable-stayed section with a 1088 m span. It is the longest cable-stayed bridge today and the first one exceeding 1000 m span in the world (Wikipedia).

A cable-stayed bridge consists of three principal components, namely girders, towers and inclined cable stays. The girder is supported elastically at points along its length by inclined cable stays so that the girder can span a much longer distance without intermediate piers. The dead load and traffic load on the girders are transmitted to the towers by inclined cables. High tensile forces exist in cable stays which induce high compression forces in towers and part of girders. The sources of nonlinearity in cable-stayed bridges mainly include the cable sag, beam-column and large deflection effects. Since high pretension force exists in inclined cables before live loads are applied, the initial geometry and the prestress of cable-stayed bridges depend on each other. Therefore the initial shape has to be determined correctly prior to analyzing the bridge. Only based on the correct initial shape, a correct deflection and vibration analysis can be achieved (Tang 1971, Morris 1974, Fleming 1979, Khalifa 1993, Au *et al.* 2001).

A lot of papers concerning analysis and construction of cable-stayed bridges have been published in last half century, but few of them concern with lateral motion of cable stays (Abdel-Ghaffar and Khalifa 1991, Pinto da Costa *et al.* 1996, Gattulli and Lepidi 2007). Abdel-Ghaffar and Khalifa (1991) indicated the importance of cable vibration and classified first finite element models of cable-stayed bridges into two catrgories: the one element cable system (OECS) and the multi-elements cable system (MECS). In the former, each cable stay is represented by a single cable (truss) element and multi-cable (truss) elements are used for each cable stay in the latter. MECS model can exhibits the lateral motion of cable stay of the bridge, but the OECS model can not. The purpose of this paper is to investigate the dynamic behaviors of cable stays of such kind of bridges. Both OECS- and MECS-models of the cable-stayed bridge are built up in the study. The MECS model is used for investigating the motion of cable stays, in which a single cable stay is represented by multi-cable elements, say 10 or 20 elements. And an efficient finite element computation procedure will be also set up for shape finding of the cable-stayed bridge with MECS model. The initial shape of the bridge with MECS model will be determined by the two-loop iteration method with the help of using catenary function for cable stay discretization. In the two-loop iteration method, the shape finding procedure is performed with both the equilibrium iteration and the shape iteration. Through equilibrium iteration, a convergent nonlinear equilibrium configuration can be achieved and through the shape iteration, a shape satisfied the requirements of architectural design can be found. The initial shape of each cable stay in MECS model is determined efficiently by using catenary function method. Based on the convergent initial shape determined, the static deflection, the vibration frequencies and modes, and seismic responses of the bridge are examined.

2. Finite element formulation of cable-stayed bridges

Based on the finite element concept, a cable-stayed bridge can be considered as an assembly of a

finite number of cable (for cable stays) and beam-column (for girder and tower) elements. In this study, some assumptions are made as follows. The material is homogeneous and isotropic. All material remains within the linear elastic range during the nonlinear responses. The external loads are displacement independent. Large displacements and large rotations are allowed, but strains are small. All cables are fixed to the tower and to the girder at their joints of attachment which are considered as frictionless hinges. The nonlinearities of cable sag, beam-column and large displacement effects are taken into consideration.

The elastic cable element possesses only tension stiffness. Under action of its own dead load and axial tensile force, a cable supported at its end will sag into a catenary shape. The axial stiffness of a cable will change with changing sag. The sag effect is taken into account by using an equivalent straight cable element with an equivalent modulus of elasticity. The concept of a cable equivalent modulus of elasticity was first introduced by Ernst (1965). If the change in tension in a cable during a load increment is not large, the axial stiffness of the cable will not change significantly and the equivalent modulus of elasticity of the cable can be considered constant during the load increment, and is given by

$$E_{eq} = \frac{E}{1 + \dfrac{(wL)^2 AE}{12T^3}}$$

in which E_{eq} = equivalent cable modulus of elasticity, E = effective cable material modulus of elasticity, A = cross-sectional area, w = cable weight per unit length, L = horizontal projected length of the cable, and T = tensile force in the cable.

The towers and part of the girders are subjected to large compression due to high pretension forces in inclined cable stays. This induces the beam-column effect and has to be taken into consideration in the cable-stayed bridge. The towers and girders are represented by an assembly of beam-columns. The beam-column element used in the paper is straight and has uniform cross section. The engineering beam theory is employed for the beam-column element and no shear strain is considered. In a beam-column element, the bending stiffness depends on the element axial forces, and the presence of bending moments will affect the axial stiffness. In general, the beam-column effect is evaluated by using the stability functions (Gimsing 1997, Fleming 1979).

Cable-stayed bridges have a larger span and less weight than those ones of conventional steel and reinforced concrete bridges. Large deflections may easily appear, hence the large displacement effect has also to be considered in the analysis, and the equilibrium equations must be set up for the deformed position. The motion of structural elements during large deflections is described by the nonlinear coordinate transformation coefficients that relate the local element coordinates to the global system coordinates (Schrader 1969, 1978, Wang *et al.* 1993, 2004, Wang and Yang 1996).

2.1 Linearized system equation

The finite element linearized system equation for a small time (or load) interval can be derived from the Lagrange's virtual work principle (Schrader 1969, 1978) as follows

$$M_{\alpha\beta}\Delta\ddot{q}^n_\beta + D_{\alpha\beta}\Delta\dot{q}^n_\beta + {}^2K^n_{\alpha\beta}\cdot\Delta q^n_\beta = \Delta P^n_\alpha + {}_uP^n_\alpha, \qquad \alpha = 1, 2, \ldots, N \text{ D.O.F.},$$
$$\text{for } t_n \le t \le t_{n+1} = t_n + \Delta t_n$$

where $M_{\alpha\beta}$ = system mass matrix, $D_{\alpha\beta}$ = system damping matrix, ${}^{2}K^{n}_{\alpha\beta}$ = tangent system stiffness matrix, ${}_{u}P^{n}_{\alpha} = P^{\alpha}_{n} - \{T^{n}_{\alpha} + D_{\alpha\beta}\dot{q}^{n}_{\beta} + M_{\alpha\beta}\ddot{q}^{n}_{\beta}\}$ = unbalanced forces in dynamics, $\Delta P^{n}_{\alpha} = P^{n+1}_{\alpha} - P^{n}_{\alpha}$ = load increments, $\Delta q^{n}_{\alpha} = q^{n+1}_{\alpha} - q^{n}_{\alpha}$ = displacement increments, and $\Delta t_n = t_{n+1} - t_n$ = time increments, P_{α} = generalized external forces, T_{α} = generalized internal forces, q_{α} = generalized system coordinates, $\dot{q}_{\alpha} = dq_{\alpha}/dt$ = generalized velocities, $\ddot{q}_{\alpha}$ = generalized accelerations, t = time, $\sum_{EL}$ = summation over all elements, and N = number of degree of freedom (D.O.F.). The subscripts $\alpha, \beta, \gamma, \ldots$ denote the number of the system coordinate. The index summation convention is used here for the subscripts. The superscript "n" denotes the number of time (or load) step, e.g., $q^{n}_{\beta} = q_{\beta}\big|_{t=t_n}$ or $q^{n}_{\beta} = q_{\beta}\big|_{P_{\alpha}=P^{n}_{\alpha}}$, and the "2" means iteration matrix of second order.

2.2 Linearized system equation in statics

In nonlinear statics, the linearized system equation becomes

$$\Delta P^{n}_{\alpha} + {}_{u}P^{n}_{\alpha} = {}^{2}K^{n}_{\alpha\beta} \cdot \Delta q^{n}_{\beta}, \quad \text{for} \quad P^{n}_{\alpha} \le P_{\alpha} \le P^{n+1}_{\alpha}$$

where ${}_{u}P^{n}_{\alpha} = P^{n}_{\alpha} - T^{n}_{\alpha}$ is the unbalanced forces at n-th load step. The linearized static system equation represents a set of linear algebraic equations and is solved step-by-step incrementally in nonlinear statics. An incremental-iteration procedure is recommended in order to get more accurate solutions.

2.3 Linear system equation in statics

In linear statics where all nonlinearities are naglected the system equation has the following linear form

$$P_{\alpha} - \overset{\circ}{T}_{\alpha} = K_{\alpha\beta} \cdot q_{\beta}$$

where $\overset{\circ}{T}_{\alpha}$ = generalized initial internal force, $K_{\alpha\beta}$ = linear constant system stiffness matrix.

3. Nonlinear analysis of cable-stayed bridges

3.1 Initial shape analysis

The initial shape of a cable-stayed bridge provides the geometric configuration as well as the prestress distribution of the bridge under action of dead loads of girders and towers, and under pretension force in inclined cable stays. The relations for the equilibrium conditions, the specified boundary conditions, and the requirements of architectural design should be satisfied.

3.1.1 Shape finding of the cable-stayed bridge with OECS model

In the OECS model of the cable-stayed bridge one element cable system (OECS) is used for cable stays, i.e., one single cable element per cable stay is used in the bridge. The single cable element is considered as a straight element including nonlinear sag effect described by the equivalent cable modulus of elasticity E_{eq} given by Ernst (1965). In most of papers published the OECS model has be used for analysis of cable-stayed bridges. The computation procedure for shape finding of the

cable-stayed bridge with OECS model by using the two-loop iteration method is briefly described in the following.

For shape finding computations, only the dead load of girders and towers is taken into account, and the dead load of cables is neglected, but cable sag nonlinearity is included. The computation for shape finding is performed by using the two-loop iteration method, i.e., equilibrium iteration and shape iteration loop. This can start with an arbitrary tension force in inclined cable stays (Wang *et al.* 1993, 2004, Wang and Yang 1996). Based on a reference configuration (the architectural designed form), having no deflection and zero prestress in girders and towers, the equilibrium position of the cable-stayed bridge under dead load is first determined iteratively (equilibrium iteration). Although the first determined configuration satisfies the equilibrium conditions and the boundary conditions, the requirements of architectural design are, in general, not fulfilled. Since the bridge span is large and no enough pretension forces exist in inclined cables, quite large deflections and bending moments may appear in the girders and towers. Another iteration then has to be carried out in order to reduce the deflection and to smooth the bending moments in members and finally to find the correct initial shape. Such an iteration procedure is named the shape iteration. The element axial forces determined in the previous step will be taken as initial element forces for the next iteration, and a new equilibrium configuration under the action of dead load and such initial forces will be determined again. During shape iteration, several control points (nodes intersected by the girder and the cable or by the tower and the cable) will be chosen for checking the convergence tolerance. In each shape iteration the ratio of the lateral displacement at control points to the main span length or tower height will be checked, i.e.

$$\left|\frac{\text{laetral displacement at control points}}{\text{main span or tower height}}\right| \le \varepsilon_s$$

The shape iteration will be repeated until the convergence tolerance ε_s, say 10^{-4}, is achieved. When the convergence tolerance is reached, the computation will stop and the initial shape of the cable-stayed bridge with OECS model is found.

The initial shape analysis can be performed in two different ways: a linear and a nonlinear computation procedure. In the linear procedure all nonlinearities of cable-stayed bridges are neglected and only the linear elastic cable, beam-column elements and linear constant coordinate transformation coefficients are used. And the shape iteration is carried out without equilibrium iteration. In the nonlinear procedure all nonlinearities of cable-stayed bridges are taken into consideration during the computation process. The nonlinear cable element with sag effect and the beam-column element including stability coefficients and nonlinear coordinate transformation coefficients are used. Both the shape iteration and the equilibrium iteration are carried out in the nonlinear computation procedure.

3.1.2 Shape finding of the cable-stayed bridge with MECS model

In the MECS model of the cable-stayed bridge multi-elements cable system (MECS) is used for cable stays, e.g., ten cable elements per cable stay are used for each cable stay in the bridge, in order to describe the lateral motion of cable stays. The weight of each cable element is lumped at the node between the elements. A convergent solution is difficult to obtain when the two-loop iteration procedure is directly used for shape finding of the bridge with MECS model. Hence the shape finding procedure of the bridge with MECS model will be carried out in a different way as follows:

Step 1: The initial shape of the cable-stayed bridge with OECS model will be first found by the procedure described in section 3.1.1, in which all the node coordinates and element preforces of the bridge are determined. From the results of the found initial shape the pretension force and the coordinates of end points of each cable stay can be picked out.

Step 2: Based on the found end node position and pretension force of each cable stay, its initial shape acted by the dead load and the pretension force will be determined by using the cable catenary function method which is briefly described in the following section 3.1.2.

Step 3: After determining the initial shape of each discretized cable stay in the MECS model by the catenary function method, all the coordinates of the interior nodes and the element preforces of cable stays are known. Then put them onto the cable-stayed bridge with the configuration determined by the OECS model and then carry out the equilibrium iteration and the shape iteration again to find its final initial shape of the MECS model.

A convergent solution can be achieved efficiently by using the computation procedure described above for finding the initial shape of the cable-stayed bridge with MECS model.

3.1.3 Catenary function method for single cable discretization

A single cable as shown in Fig. 1, is discretized into n straight segments with $n+1$ nodes. The cable weight is lumped at the nodal points with the magnitude of W_i for the i-th node. The coordinates of the i-th node are denoted as (X_i, Y_i), where $i = 1, 2, 3, \ldots, n+1$. The horizontal preforce H is given. The initial shape of a discrete cable can easily determined by the method of joints in statics, but large numerical error may appear when the cable is not fine enough discretized.

Here, a more accurate (quasi-exact) method, the catenary function method, for finding the initial shape and pre-stress distribution of a discrete cable under its own weight will be presented. The advantage of this method is accurate and highly efficient, in which no simultaneous equations solving and no iteration are required during shape finding of cables. For a single cable, the analytical solution for its shape is a catenary under the conditions of no axial deformation and the assumption of uniform body weight. Here, we directly use the analytical solution of a cable catenary and perform numerical analysis to obtain the initial shape of a single discrete cable. Assume the horizontal perforce H and the uniformly distributed body weight of the cable denoted as $w(s) = w$ = constant are given, where s is the *arc*-length. The shape of the cable is described by a catenary function (Ernst 1965) as

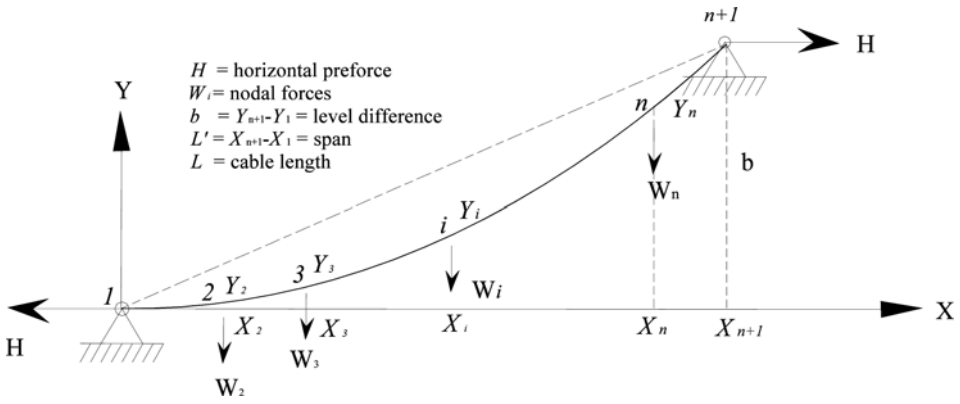

Fig. 1 Schematic of a discrete cable

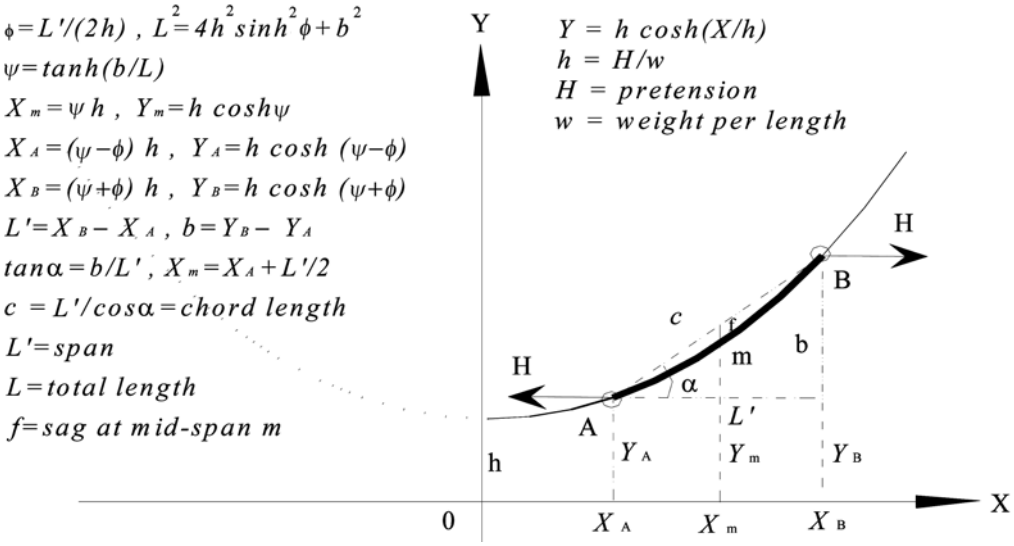

Fig. 2 Catenary function

$$Y = h\cosh(X/h)$$

where $h = H/w$ = ordinate of the apex of the catenary function, H = horizontal preforce and w = weight per length of the cable. Let's assume the cable AB is hinged at point A and B with a span L', and the level difference between the two ends is b. To determine the positions of A and B of the cable on a catenary in Fig. 2, we define two dimensionless parameters ϕ, ψ to describe the relationship between the horizontal projection of L' and h, and the relationship between coordinate of the midpoint of the span X_m and h, respectively, i.e.

$$\psi = X_m/h \quad \text{and} \quad \phi = L'/2h$$

When w, H, L' and b are given, $h = H/w$ and $\phi = L'/2h$ are known, but not ψ. The value of ψ has to be first determined as follows. Since $X_m = \psi h$, $L' = 2h\phi$, and $Y_m = h\cosh\psi$, the location of the end points A, B of the cable on the catenary curve can be expressed as

$$X_A = X_m - L'/2 = (\psi - \phi)h, \quad X_B = X_m + L'/2 = (\psi + \phi)h$$
$$Y_A = h\cosh(\phi - \psi), \qquad Y_B = h\cosh(\phi + \psi)$$

The level difference between the end supports is

$$b = Y_B - Y_A = h[\cosh(\psi + \phi)h - \cosh(\psi - \phi)h] = 2h\sinh\psi\sinh\phi$$

Since $Y = h\cosh(X/h)$, $dY/dX = \sinh(X/h)$, the total length of the cable is obtained by integration

$$L = \int ds = \int_{X_A}^{X_B} \sqrt{1 + (dY/dX)^2}\, dX$$
$$= \int_{(\psi-\phi)h}^{(\psi+\phi)h} \sqrt{1 + \sinh^2(X/h)}\, dx = [h\sinh(X/h)]_{(\psi-\phi)h}^{(\psi+\phi)h}$$
$$= h[\sinh(\psi + \phi) - \sinh(\psi - \phi)] = 2h\cosh\psi\sinh\phi$$

Divide L by b, one obtains $\tanh\psi = b/L$,and $\psi = \tanh^{-1}(b/L)$, where $L = [b^2 + 4h^2\sinh^2\phi]^{1/2}$ is calculated from $L^2 - b^2 = 4h^2\sinh^2\phi$.

After determining $\psi = \tanh^{-1}(b/L)$, the coordinates of the midpoint m and end points A, B of the cable on the catenary are found here.

$$X_m = \psi h, \quad Y_m = h\cosh\psi$$
$$X_A = X_m - L'/2 = (\psi - \phi)h, \quad X_B = X_m + L'/2 = (\psi + \phi)h$$
$$Y_A = h\cosh(\phi - \psi), \qquad Y_B = h\cosh(\phi + \psi)$$

The following items of the cable AB are determined:

Angle for the inclined chord of the cable AB $\quad \alpha = \tan^{-1}(b/L')$

Chord length c of the cable AB $\quad c = \sqrt{(L')^2 + b^2} = L'/\cos\alpha$

Sag of the cable AB

Here, we define the sag of the cable is the vertical distance between the cable and its chord at the midspan. And the sag is calculated through

$$f = \frac{1}{2}b - (Y_m - Y_A)$$

Assume that the horizontal projection of each element has the same length, i.e., $\Delta X_i = L'/n$, and let $X_1 = X_A, Y_1 = Y_A, X_{n+1} = X_B, Y_{n+1} = Y_B$

The coordinates for interior nodes become

$$X_{i+1} = X_i + \Delta X_i \qquad i = 1, 2, \ldots, n$$
$$Y_i = h\cosh(X_i/h) \quad i = 1, 2, \ldots, n+1$$

Horizontal and vertical projected length of elements

$$\Delta X_i = X_i - X_{i-1}, \quad \Delta Y_i = Y_i - Y_{i-1} \qquad i = 1, 2, \ldots, n$$

Length of elements $\quad l_i = \sqrt{(\Delta X_i)^2 + (\Delta Y_i)^2}, \quad i = 1, 2, \ldots, n$

Inclined angle of elements $\quad \theta_i = \tan^{-1}(\Delta Y_i/\Delta X_i), \quad i = 1, 2, \ldots, n$

Internal force of elements $\quad S_i = H/\cos\theta_i, \quad i = 1, 2, \ldots, n$

Equivalent load at nodes $\quad W_i \cong \frac{1}{2}(l_i + l_{i-1}) \cdot w, \quad i = 1, 2, \ldots, n$

Total length of the cable $\quad L \cong \sum_{i=1}^{n} l_i$

Total weight of the cable $\quad W \cong \sum_{i=1}^{n} W_i$

Assume that the left end support of the cable AB locates at the origin of the coordinate system used, then one needs to perform translational transformation to obtain the actual coordinates for each node of the cable.

$$X_i = X_i - X_A, \; Y_i = Y_i - Y_A, \qquad i = 1, 2, \ldots, n+1$$

3.2 Static deflection analysis

Based on the determined initial shape, the nonlinear static deflection analysis of cable-stayed bridges with OECS- and MECS-models under live load can be performed incrementwise or iterationwise. An increment-iteration procedure is highly recommended, in which the load will be incremented, and the iteration will be carried out in each load step. Newton-Raphson iteration procedure is employed in the paper.

3.3 Vibration frequency analysis

Based on the concept of linearized vibration the natural frequencies and modes of cable-stayed bridges are examined. In the linearized vibration, the system vibrate with small amplitude around a certain nonlinear static state, where the change of the nonlinear static state induced by the vibration is small and negligible. For the cable-stayed bridge, its initial shape is the nonlinear static state q_α^A. Based on the nonlinear static state q_α^A the system matrices are established and the linearized system equation has the form as follows

$$M_{\alpha\beta}^A \ddot{q}_\beta + D_{\alpha\beta}^A \dot{q}_\beta + {}^2K_{\alpha\beta}^A \cdot q_\beta = P_\alpha(t) - T_\alpha^A$$

where the superscript "A" denotes the quantity calculated at the nonlinear static state q_α^A. This equation represents a set of linear ordinary differential equations of second order with constant coefficient matrices $M_{\alpha\beta}^A, D_{\alpha\beta}^A$ and ${}^2K_{\alpha\beta}^A$. When damping effect and load terms are neglected, the system equation of free vibration becomes

$$M_{\alpha\beta}^A \ddot{q}_\beta + {}^2K_{\alpha\beta}^A \cdot q_\beta = 0$$

The natural vibration frequencies and modes can be obtained from the above equation by using eigensolution procedures, e.g., transformation methods or subspace iteration methods (Wilkinson and Reinsch 1971). When the cable-stayed bridge vibrates with small amplitude based on the initial shape, the natural frequencies and modes can be found by solving the above equation.

4. Symmetric harp cable-stayed bridge

The symmetric harp cable-stayed bridge is taken from Tang (1971) with a modified form of cantilever supported towers as shown in Fig. 3. Its geometric and physical properties are also given in the figure. As shown in Fig. 4, the bridge with OECS model consists of NE = 34 elements (12 cable elements and 22 beam-column elements for girder and tower), NJ = 23 nodes, NU = 69 D.O.F. and the semi-band width of the system matrix ISB = 21. In the bridge with MECS model, ten cable elements per cable stay are used and the MECS model has NE = 142 (120 cable elements and 22 beam-column elements), NJ = 131, NU = 285 and ISB = 243.

4.1 Initial shape analysis

The initial shape of the bridge with OECS- and MECS-models are first determined by using two-loop iteration method with help of the catenary function method described in previous section and plotted in Fig. 5. It is obviously seen in Fig. 5 that the sagged shape of cable stay appears in the

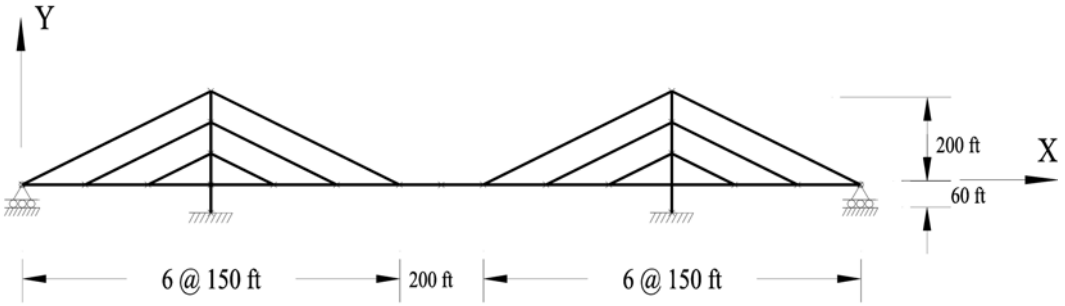

girder, tower		E = 4,320,000 ksf
cable		E = 4,320,000 ksf
girder		I = 131.0 ft^4, A=3.44 ft^2
tower		I = 24.4, 40.0, 50.0, 60.0 ft^4 (from top to buttom)
		A = 2.18, 2.45, 2.90, 3.20 ft^2
cable		exterior : A = 0.452 ft^2
		interior : A = 0.174 ft^2
dead load	girder :	w = 6.0 kips/ft , ρ = 0.05417 slug/ft^3
	cable : exterior	w = 0.221 kips/ft , ρ = 0.01518 slug/ft^3
	interior	w = 0.085 kips/ft , ρ = 0.01518 slug/ft^3

Fig. 3 Symmetric harp cable-stayed bridge

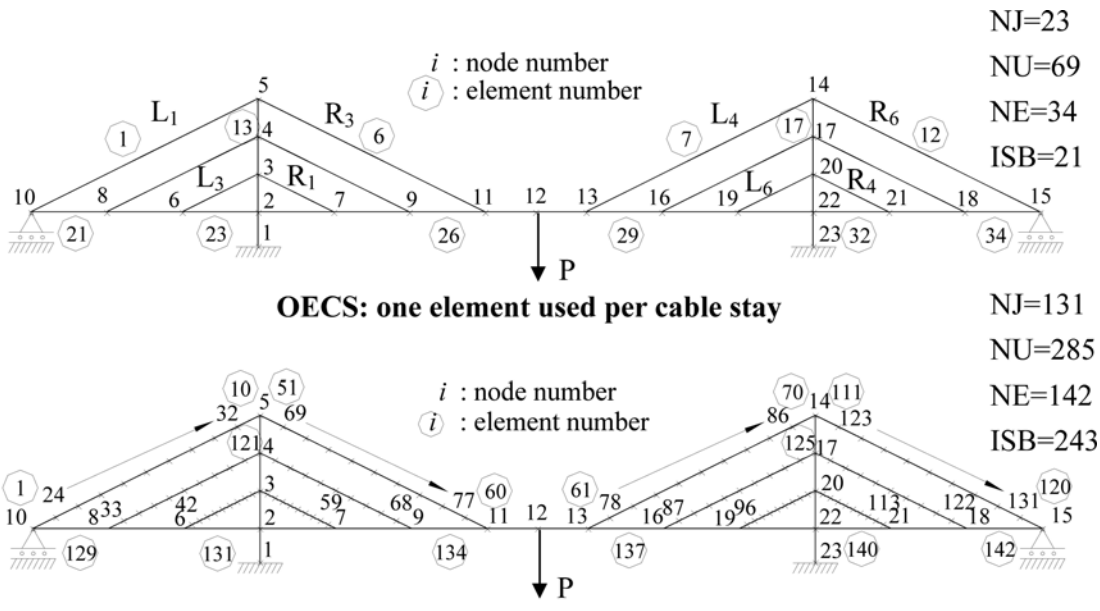

L_i : i-th cable stay from exterior to interior in side span

R_i : i-th cable stay from interior to exterior in main span

Fig. 4 Node and element numbering of harp cable-stayed bridge

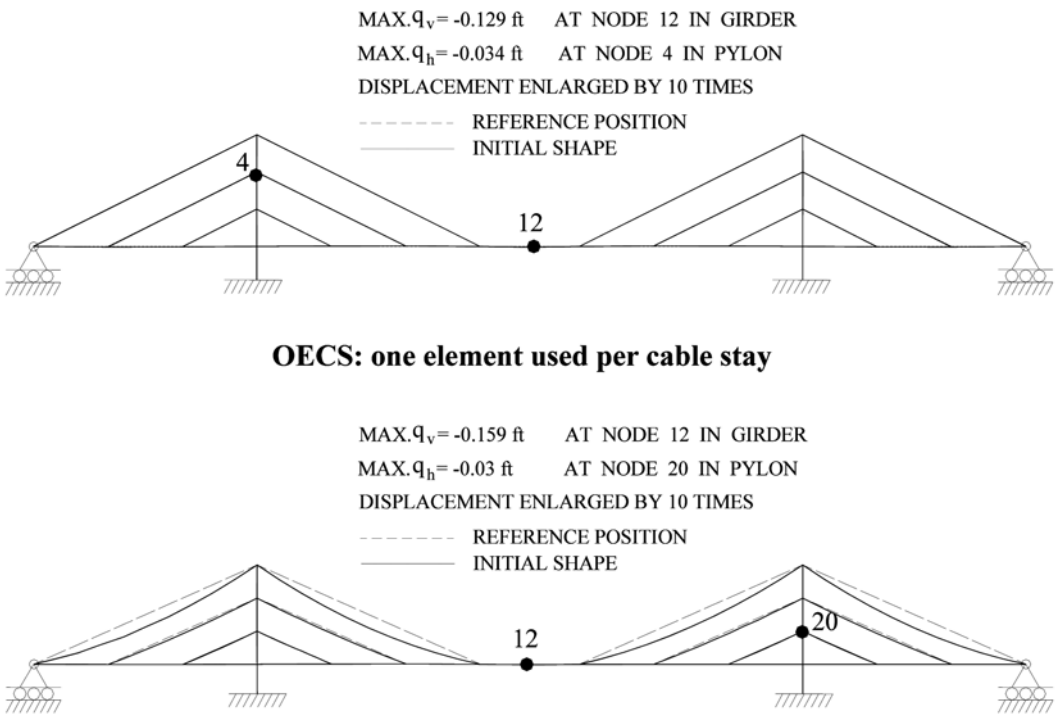

Fig. 5 Initial shape of harp cable-stayed bridge

MECS model, while the cable stay is straight in the OECS model.

4.1.1 Shape finding of the bridge with OECS model

The shape finding procedure described in section 3.1.1 is performed for the harp cable-stayed bridge with OECS model. A convergence tolerance $\varepsilon = 10^{-4}$ is used for both the equilibrium iteration and the shape iteration. The nodes of number 7, 9, 12, 16, 19 on the girder and number 5, 14 on the tower are chosen as the control points for checking the convergence tolerance. Convergent initial shape is obtained and plotted in Fig. 5, where cable stays are straight. The deflection of girder and tower measured from the architectural designed position has relatively small values, i.e., maximum vertical displacement q_v = −0.129 ft in girder and maximum horizontal displacement q_h = −0.034 ft in tower. The shape finding computation converges rapidly and four times of shape iteration is performed.

4.1.2 Shape finding of the bridge with MECS model

The shape finding procedure described in section 3.1.2 is performed for the harp cable-stayed bridge with MECS model as follows:

Step 1: Shape finding of the bridge with OECS model is done first by the procedure described in section 3.1.1.

Step 2: Shape finding of each single cable stay

The pretension force and coordinates of end nodes in each cable stay are picked out from

the results obtained in step 1. Then the initial shape of each single cable stay represented by multi-elements are determined one by one by using the catenary function method described in section 3.1.3.

Step 3: Shape finding of the bridge with MECS model

One can put the determined pretension force, coordinates and nodal load of interior nodes of each cable stay into the bridge with MECS model, and carry out again the equilibrium and shape iterations for finding the final convergent initial shape of the bridge. In this step, only one shape iteration is required to get the final convergent solution and the final initial shape of the bridge with MECS model is plotted in Fig. 5. In Fig. 5, it can be seen that the maximum deflection measured from architectural designed position is about $q_v = -0.159$ ft in girder and $q_h = -0.03$ ft in tower, and the sagged shape of cable stays can obviously be observed.

4.2 Static deflection analysis

Based on the convergent initial shape, the static deflection is examined. The static deflection of the harp cable-stayed bridge under a concentrated load P at mid-span is determined by incremental-iteration procedure using the Newton-Raphson method. The load-deflection curves determined with the OECS- and MECS-models are plotted in Fig. 6, where the vertical load P is positive when it acts downwards, and the vertical deflection is positive when it displaces upwards. When the load acts downwards, the deflections at mid-span have almost the same value for both OECS- and MECS-models. When the load acts upwards and increases till $P = -2700$ kips, the deflections determined by both models have the same value, however, when P exceeds -2700 kips, small deviation in the deflection curves can be seen in Fig. 6. The slackness of cable stay R_3 occurs at about $P = -2700$ kips and the axial force in cable stay R_1 approaches zero when $P = -6000$ kips, see the load-element force curve in Fig. 7. The member forces in girder element 135 at mid-span and

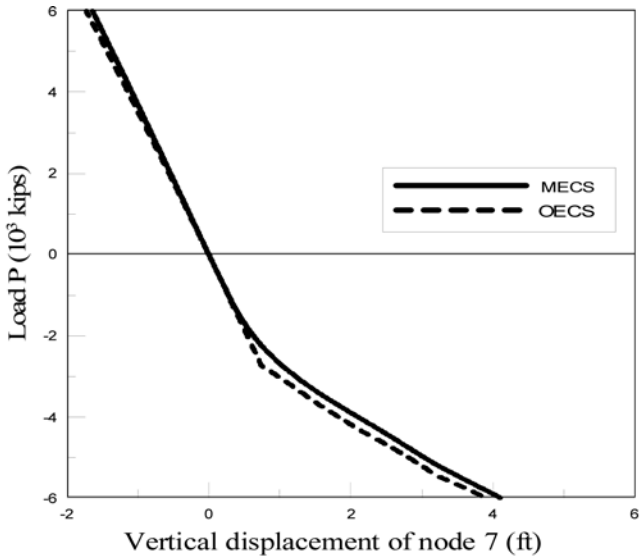

Fig. 6 Load-deflection curve of harp cable-stayed bridge

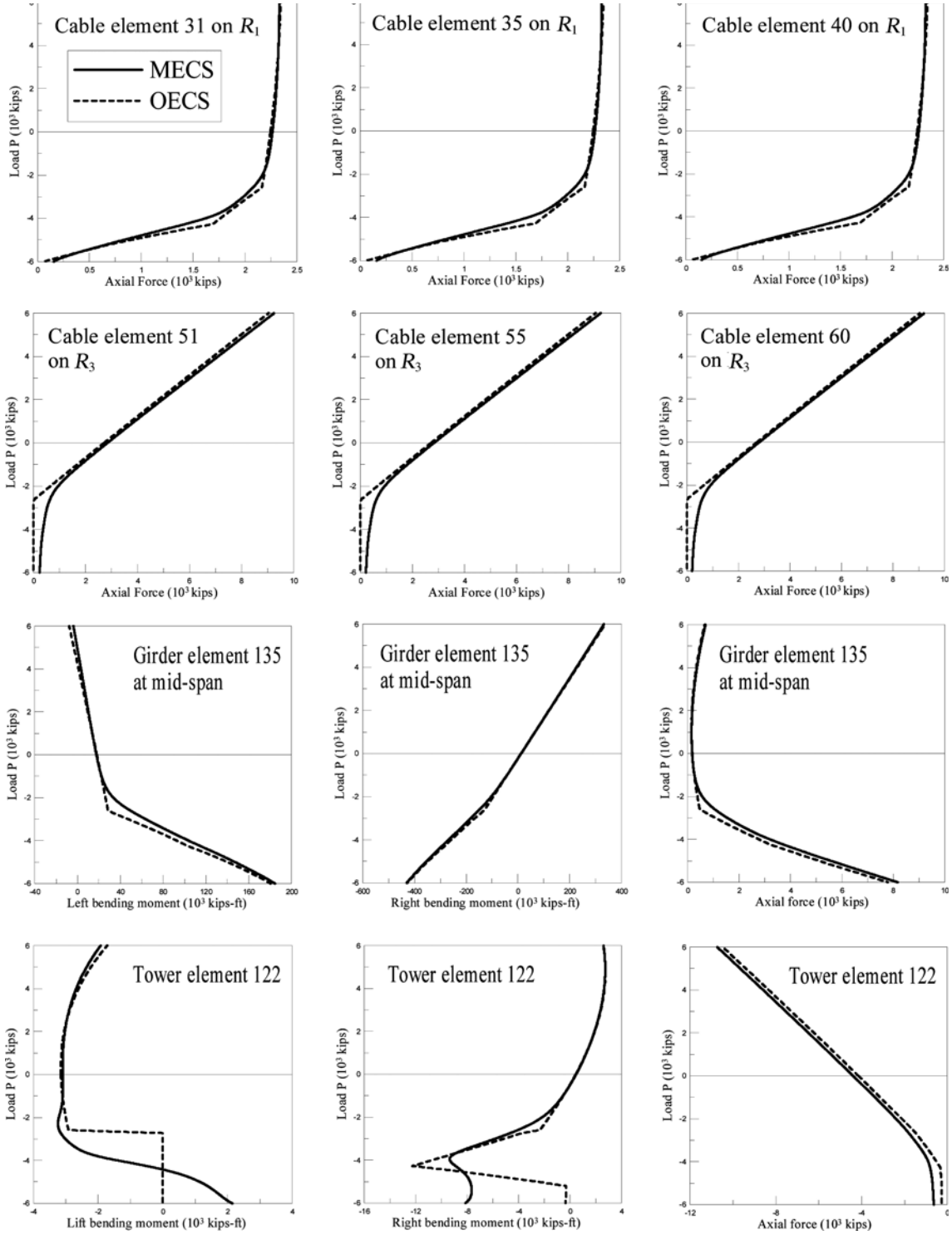

Fig. 7 Load-element force curve of harp cable-stayed bridge

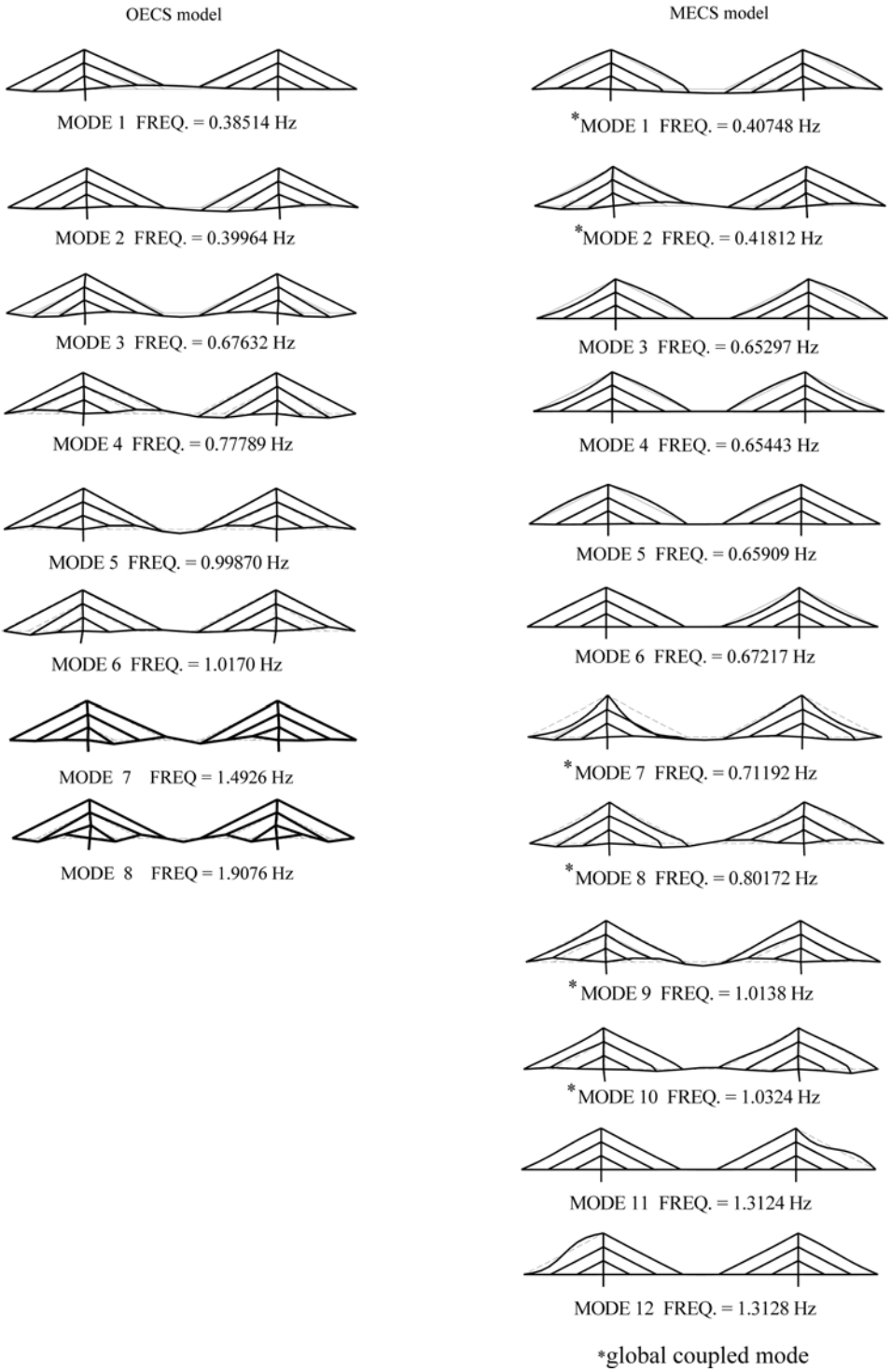

Fig. 8 Vibration frequencies and modes of harp cable-stayed bridge (OECS: one element used per cable stay, MECS: ten elements used per cable stay)

tower element 122 between nodes 3 and 4 are also plotted in Fig. 7. After the slackness of cable stay R_3 occurs, the results of both OECS- and MECS-models deviate slightly from each other and large difference appears only in bending moment of tower element 122.

4.3 Vibration frequency analysis

Based on the convergent initial shapes determined, the natural vibration frequencies and modes are examined by using OECS- and MECS-models. The frequencies and mode shapes of the first 8 modes of OECS model and the first 12 modes of MECS model are found by the Rutishauser method (Wilkinson and Reinsch 1971) and shown in Fig. 8.

4.3.1 Vibration modes of the bridge with OECS model

The first 8 modes of the harp cable-stayed bridge with OECS model are shown in Fig. 8. All the modes exhibit the global mode of girder and tower motion without motion of cable stays. Most of them are the coupled mode of girder and tower. The vibration frequencies are between 0.3851 Hz. to 1.9076 Hz from modes 1 to 8.

4.3.2 Vibration modes of the bridge with MECS model

The first 12 modes of the harp cable-stayed bridge with MECS model are determined and plotted in Fig. 8, in which modes 1, 2, 7, 8, 9, 10 exhibit the global mode of the bridge and are corresponding to modes 1 to 6 of OECS model. All the global modes of MECS model exhibit coupled motion of cable stays, girder and tower. The global coupled modes are marked with star * in Fig. 8. They are listed in Table 1 with the results of OECS model for comparison. The vibration frequencies of the global modes of MECS model are between 0.4075 Hz to 1.3128 Hz. The frequency values have a little bit larger than that of OECS model and have a difference of 6% in mode 1 and 2.2% in mode 7. It may be explained that the use of cable equivalent modulus of elasticity E_{eq} causes an over reduction of the axial stiffness of cable stays. All the modes except the global modes mentioned above belong to local mode of cable stay motion, i.e., modes 3, 4, 5, 6 of MECS model in Fig. 8. The mode 11, 12 exhibits the second cable mode of cable stay R_6 and L_1 on side span. It has been seen that the MECS model can offer all the vibration modes of the bridge including the global coupled modes and the local modes of cable stays, while the bridge with OECS

Table 1 Natural frequencies and mode shapes of global modes of harp cable-stayed bridge

OECS model			MECS model		
Mode No.	Frequency (Hz)	Mode Shape Dominated by Transversal Motion of	Mode No.	Frequency (Hz)	Mode Shape Dominated by Transversal Motion of
1	0.3851	Tower and Girder	1	0.4075	Tower, Girder and Cable Stays
2	0.3996	Same as above	2	0.4181	Same as above
3	0.6763	Same as above	7	0.7119	Same as above
4	0.7779	Same as above	8	0.8017	Same as above
5	0.9987	Same as above	9	1.0138	Same as above
6	1.0170	Same as above	10	1.0324	Same as above
7	1.4926	Same as above			
8	1.9076	Same as above			

model can only offers the global modes with girder and tower motion of the bridge, but not the local modes of cable stays.

4.4 Seismic analysis

The nonlinear dynamic responses of the harp cable-stayed bridge under uniform seismic excitation will be examined here. The accelerogram of Chi-chi earthquake, recorded at Shih-Gang station No. TCU068 on September 21, 1999 in Taiwan (Lee *et al.* 2001), as shown in Fig. 9, is taken as the input data of seismic loading. Only the strong part from the period of 30 to 60 sec. of the vertical component of the accelerogram is used, in which the maximum and minimum acceleration are 498.96 gal and −279.73 gal, respectively. The nonlinear dynamic responses are determined by using the Newmark-$\beta = 1/4$ direct integration method, where the time step size $\Delta t = 0.001$ sec. is used, the total number of time steps is NT = 30000, and no damping is considered.

The displacement responses of the bridge with both OECS- and MECS-models are plotted in Figs. 10 and 11. The dynamic displacement responses of cable stays can only be determined in the bridge with MECS model. Three nodal displacement responses of the most exterior cable stays L_1 and R_3 are shown in Fig. 10, where nodes 28, 73 are the mid-point of the cable stay L_1, R_3, respectively. The vertical displacement response has the maximum value approaching 4 ft occurred at the mid-point of the most exterior cable stay L_1 and R_3. The nodal displacement responses of girder and tower determined by both OECS- and MECS-models are plotted in Fig. 11. Both response curves of OECS- and MECS-models agree well with each other and have no great difference. The nodes 5 and 14 are located at the top of the towers and the maximum horizontal displacement at tower top approaches 0.8 ft. The nodes 8, 11, 12 and 13 are on the girder and have maximum vertical displacement about 3.38 ft at node 12 on the mid-point of the girder.

The dynamic cable force responses of cable stays L_1 and R_3 for both OECS- and MECS-models are plotted in Fig. 12. The bridge with OECS model offers only a mean value of axial force in cable stays and its cable force response is plotted with dash line in Fig. 12. The element axial force responses obtained in the bridge with MECS model are plotted with solid line in Fig. 12, in which the axial force of three cable elements located at one fourth of length of the cable stay L_1, R_3 are shown. The results show the variation of axial force along the cable stay is small. The maximum

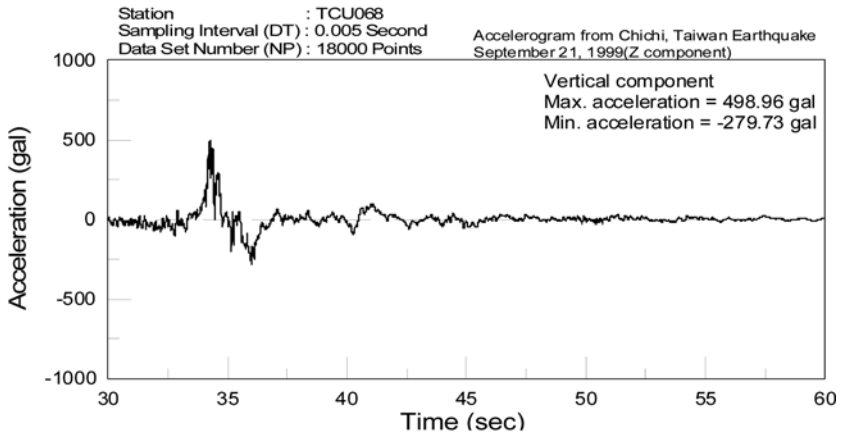

Fig. 9 Ground acceleration history of Chi-chi earthquake (Station No. TCU068)

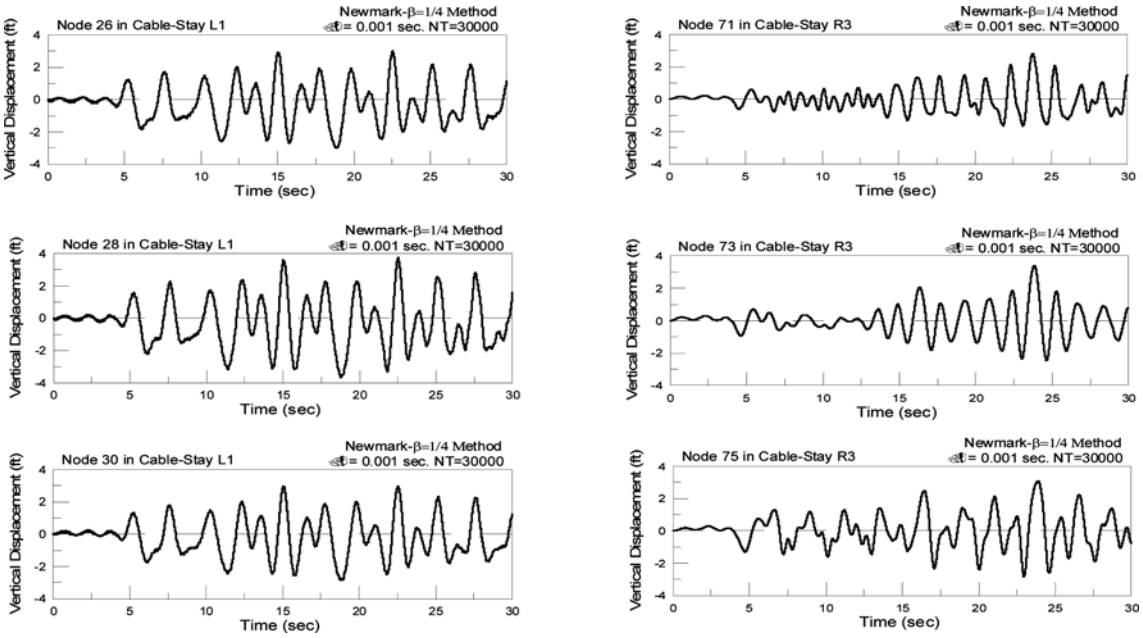

Fig. 10 Displacement response of cable stays of harp cable-stayed bridge under vertical seismic excitation (MECS: ten elements used per cable stay)

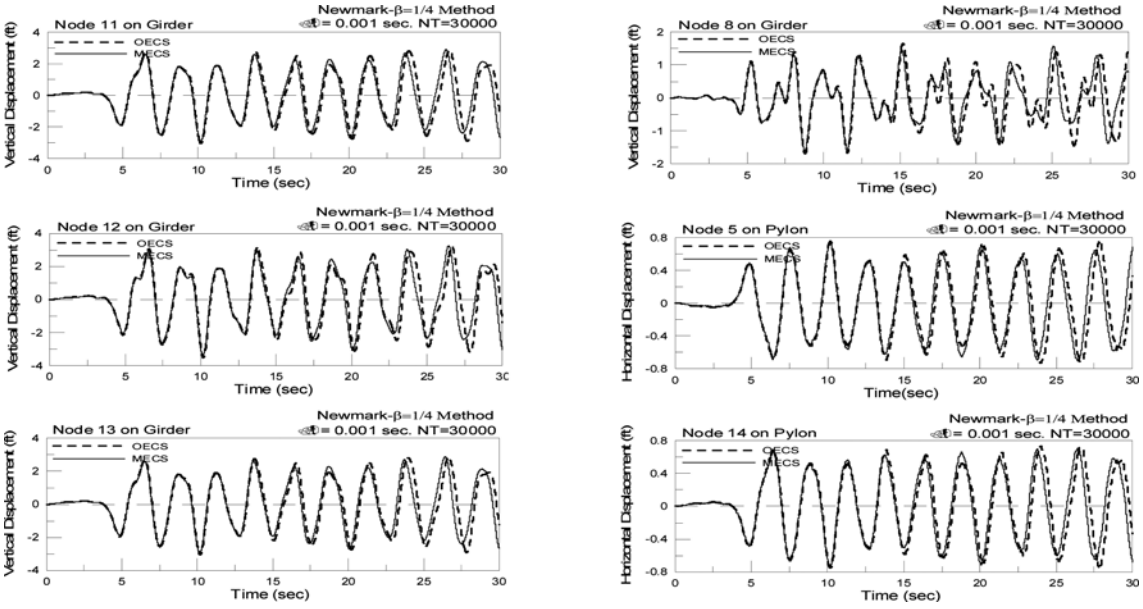

Fig. 11 Displacement response of girder and tower of harp cable-stayed bridge under vertical seismic excitation (OECS: one element used per cable stay, MECS: ten elements used per cable stay)

axial force appear in the most exterior cable stay L_1 and has the value of 4.833×10^3 kips. The dynamic member force responses of tower element 16 between nodes 1 and 2 and girder element

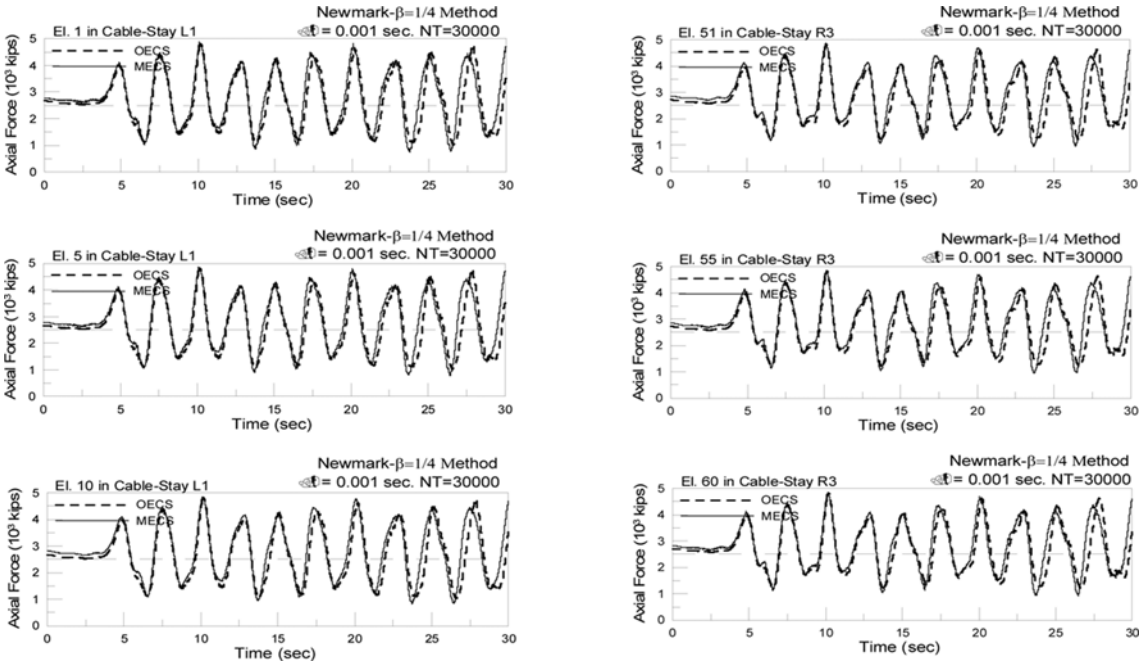

Fig. 12 Member force response of cable stays of harp cable-stayed bridge under vertical seismic excitation (OECS: one element used per cable stay, MECS: ten elements used per cable stay)

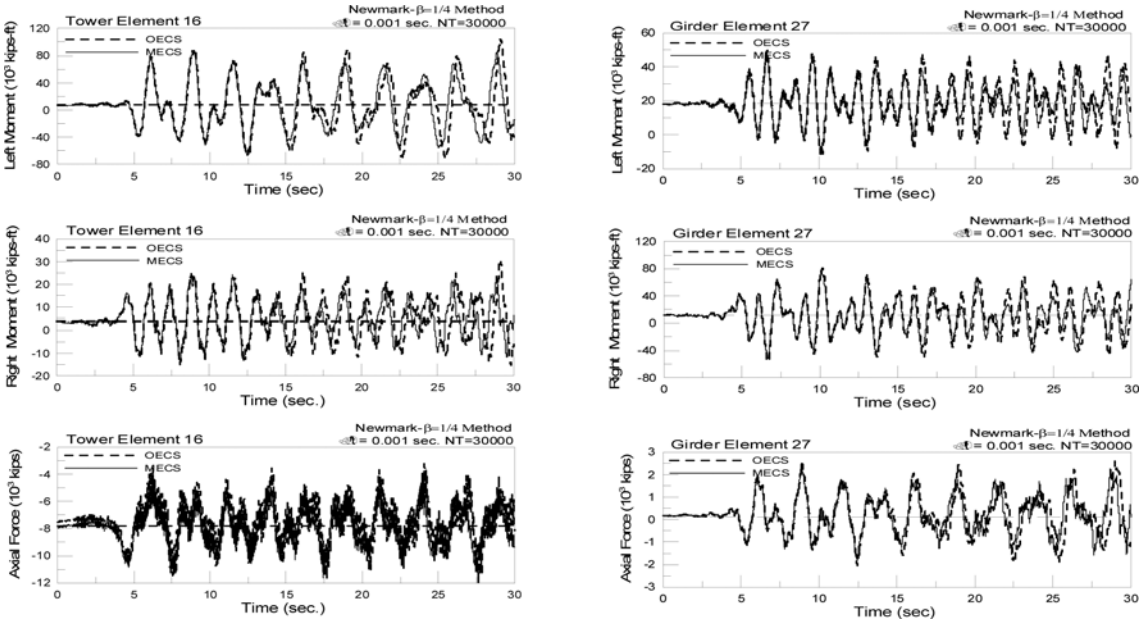

Fig. 13 Member force response of girder and tower of harp cable-stayed bridge under vertical seismic excitation (OECS: one element used per cable stay, MECS: ten elements used per cable stay)

27 between nodes 11 and 12 in OECS model are plotted in Fig. 13. The results determined by both models agree well with each other and have no great difference.

5. Conclusions

Two analytical models for the cable stay system of cable-stayed bridges are built up in the study. One is the OECS (one element cable system) model in which one single element per cable stay is used and the other is MECS (multi-elements cable system) model, where multi-elements per cable stay are used. A finite element computation procedure has also been set up for the nonlinear analysis of such kind of structures including initial shape, static deflection, vibration frequency and seismic analysis. The dynamic structural behaviors of the bridge influenced by the cable vibration have also been examined by the MECS model. Based on numerical experiments in the study, some conclusions are summarized as follows:

1. The two-loop iteration method can be well used for shape finding of cable-stayed bridges with the MECS model as it is conventionally used in the OECS model, and a converged initial shape can be found efficiently.
2. The catenary function method works efficiently for shape finding of individual cable stays in the bridge of MECS model. With its help, a convergent initial shape of the bridge of MECS model can be easily determined. The MECS model offers the real sagged shape of cable stays in initial shape analysis.
3. The results of static deflection analysis determined by the OECS- and MECS-models are almost the same. Attention must be paid only, when the slackness of cable stays occurs, slight deviation will appear between the results determined by both models. The OECS model works much more efficiently in general, and is accurate enough for static deflection analysis of cable-stayed bridges.
4. The results of vibration frequency analysis show that the modes of cable-stayed bridges consist of global modes and local modes. The global mode of the bridge consists of coupled girder, tower and cable stays motion and is a coupled mode, while the local mode exhibits only the motion of cable stays and is uncoupled with girder and tower.
5. The MECS model offers all modes of the bridge including global modes and local modes in vibration frequency analysis. The OECS model offers only the global modes, but no local modes of cable stays.
6. In the nonlinear seismic analysis, only the MECS model can offer the lateral displacement response of cable stays and the axial force variation in cable stays. The responses of towers and girders of the bridge determined by both OECS- and MECS-models have no great difference.
7. The MECS model is much more time consuming than OECS model, especially in nonlinear dynamic response analysis. For only investigating the global girder and tower behaviors of cable-stayed bridges, the OECS model performs well enough and is much more computationally efficient.

Acknowledgements

The research was sponsored by a grant under No. NSC 92-2211-E-033-009, form the National Science Council, Taiwan, R.O.C.

References

Abdel-Ghaffar, A.M. and Khalifa, M.A. (1991), "Importance of cable vibration in dynamics of cable-stayed bridges", *J. Eng. Mech-ASCE*, **117**(11), 2571-2589.

Au, F.T.K., Cheng, Y.S., Cheung, Y.K. and Zheng, D.Y. (2001), "On the determination of natural frequencies and mode shapes of cable-stayed bridges", *Appl. Math. Model.*, **25**(12), 1099-1115.

Ernst, H.J. (1965), "Der E-Modul von Seilen unter Beruecksichtigung des Durchhanges", *Der Bauingenieur* **40**(2), 52-55 (in German).

Fleming, J.F. (1979), "Nonlinear static analysis of cable-stayed bridge structures", *Comput. Struct.*, **10**(4), 621-635.

Gattulli, V. and Lepidi, M. (2007), "Localization and veering in the dynamics of cable-stayed bridges", *Comput. Struct.*, **85**(21-22), 1661-1678.

Gimsing, N.J. (1997), *Cable Supported Bridges: Concept and Design*, 2nd edition, John Wiley & Sons Ltd., Chichester.

Khalifa, M.A. (1993), "Parametric study of cable-stayed bridge response due to traffic-induced vibration", *Comput. Struct.*, **47**(2), 321-339.

Lee, W.H.K., Shin, T.C., Kuo, K.W., Chen, K.C. and Wu, C.F. (2001), "CWB free-field strong-motion data from the 21 September Chi-Chi, Taiwan, Earthquake", *B. Seismol. Soc. Am.*, **91**(5), 1370-1376.

Leonhardt, F. and Zellner, W. (1991), "Past, present and future of cable-stayed bridges", *Proceedings of the Seminar of Cable-Stayed Bridges: Recent Developments and Their Future*, Yokohama, December.

Morris, N.F. (1974), "Dynamic analysis of cable-stiffened structures", *J. Struct. Div-ASCE*, **100**(5), 971-981.

Pinto da Costa, A., Martins, J.A.C., Branco, F. and Lilien, J.L. (1996), "Oscillations of bridge stay cables induced by periodic motions of deck and/or towers", *J. Eng. Mech-ASCE*, **122**(7), 613-622.

Schrader, K.H. (1969), Die Deformationsmethode als Grundlage einer Problemorientierten Sprache, BI-Taschenbuch, 830, Bibliographisches Institute, Mannheim, Zurich.

Schrader, K.H. (1978), MeSy Einfuehrung in das Konzept und Benutzeranleitung fuer das Programm MESY-MINI, Technisch-Wissenschaftliche Mitteilung Nr. 78-11, Institut Fuer Konstruktiven Inginieurbau, Ruhr-Universitaet Bochum.

Tang, M.C. (1971), "Analysis of cable-stayed girder bridges", *J. Struct. Div-ASCE*, **97**(5), 1481-1496.

Wang, P.H. and Yang, C.G. (1996), "Parametric studies on cable-stayed bridges", *Comput. Struct.*, **60**(2), 243-260.

Wang, P.H., Tang, T.Y. and Zheng, H.N. (2004), "Analysis of cable-stayed bridges during construction by cantilever methods", *Comput. Struct.*, **82**(4-5), 329-346.

Wang, P.H., Tseng, T.C. and Yang, C.G. (1993), "Initial shape of cable-stayed bridges", *Comput. Struct.*, **46**(6), 1095-1106.

Wilkinson, J.H. and Reinsch, C. (1971), *Handbook for Automatic Computation*, Vol. 2, Linear Algebra (Eds. Householder, A.S. and Bauer, F.L.), Springer Verlag, New York.

Wikipedia, http://en.wikipedia.org/wiki/cable-stayed_bridge